

Journal of Environmental Science and Technology

ISSN 1994-7887





Journal of Environmental Science and Technology 7 (6): 314-325, 2014 ISSN 1994-7887 / DOI: 10.3923/jest.2014.314.325

© 2014 Asian Network for Scientific Information

Simulation of Scouring in Front of an Impermeable Vertical Breakwater Using the RANS-VOF Numerical Model

¹N. Tofany, ²M.F. Ahmad, ³M. Mamat and ¹M.L. Husain

Corresponding Author: M.F. Ahmad, Department of Maritime Technology, School of Ocean Engineering, University Malaysia Terengganu, Malaysia

ABSTRACT

This study presents the application of the RANS-VOF based model for scouring simulation with different wave condition in front of vertical breakwater. An empirical sediment transport formulae of Bailard (1981) was applied to estimate the bed profile change. Additional terms of bottom shear stress were included in the momentum equations and surprisingly seem necessary to produce a physical scouring/deposition pattern. Validation results showed that the present model is very accurate in the prediction of near bottom velocity. The numerical bed-profile was also consistent to experimental data. It was observed that different wave conditions produce standing waves with different characteristics in front of the breakwater. This consequently develops different scouring pattern at the bottom. As the size of incoming wave increases, the size of scouring trough and deposition ridges also increase.

Key words: RANS-VOF numerical model, sediment transport, scouring, standing waves, wave conditions

INTRODUCTION

Scouring is a common side-effect that appears in the functionality of breakwaters for coastal protection. It is a bed profile change mechanism that possibly threatens stability of breakwater/other coastal structures as reported by Irie and Nadaoka (1984) and Takahasi (2002). Serious effects of scouring have triggered the European Union (EU) countries to extensively study scouring around coastal structures through the Marine Science and Technology (MAST) program. This program involved nine research institutions from six European countries which collaborated under the project of Scour Around Coastal Structures (SCARCOST). Sumer et al. (2001) provided a summary of the results of this project. Prediction of scouring is now still an active research topic among researchers and coastal engineers.

Wave condition is one of main factors in the development of scouring. However, in many situations, experiments might be constrained to give a complete description of the wave condition effects due to many limiting factors. Analytical solutions might also not be able to describe physical phenomenon with high degree of complexity. These problems have triggered many researchers to study scouring by using numerical models, such as Gislason *et al.* (2009), Hajivalie and

¹Institute of Oceanography and Environment, University Malaysia Terengganu, Malaysia

²School of Ocean Engineering, University Malaysia Terengganu, Malaysia

³Faculty of Informatics and Computing, University Sultan Zainal Abidin, Malaysia

Yeganeh-Bakhtiary (2009), Tahersima et al. (2011) and Hajivalie et al. (2012). Numerical studies have been proven giving advances in the knowledge of hydrodynamics and scouring in front of impermeable breakwater.

In numerical approach, the models based on Reynold Averaged Navier-Stokes (RANS) equations and Volume of Fluid Method (VOF) seem promising to capture the details of wave-structure-sediment interactions. These models are mostly in the framework of one-phase approach that is combined with a morphological model. The morphological model generally consists of the continuity equation for sediment (Fredsoe and Deigaard, 1992) and the bed-load equation of Engelund and Fredsoe (1976). In the one-phase approach, the interaction of fluid and sediment at the bottom is assumed to occur only one-way, only the fluid that influences the sediment motion. Then, the bed profile change is estimated using empirical formula. This approach is relatively enough to capture the bed profile change and tend to be simpler and more practical to apply than the two-phase approach as used by Hajivalie et al. (2012).

Unlike the existing one-phase models, this study will present the application of the RANS-VOF based model that is combined with an empirical sediment transport formula of Bailard (1981) for simulations of scouring in front of a vertical breakwater. Additional bottom shear stress terms as used by Karambas (1998) were included in the momentum equations. Surprisingly, it was found that these terms might be necessary to produce physical scouring/deposition patterns. Unfortunately, none of the aforementioned one-phase models has taken these terms into account.

After comparing with the previous study (Tahersima et al., 2011) results of the present model tend to show better consistency of scouring/deposition patterns with the experimental result of Xie (1981). Further, a systematic analysis will be presented regarding the effects of different wave conditions to the scouring pattern that form at the bottom. The modeling approach and results given in the present study are intended as a contribution to the current stage knowledge of scouring simulations.

NUMERICAL MODEL

The SOLA-VOF code (Nichols *et al.*, 1980) was modified by adding some additional features to be more suitable for simulating the wave-structure-sediment interactions. The main components of the present model are presented in numerical model.

Governing equations: The governing equations were based on The Reynolds Averaged Navier-Stokes (RANS) equations which were combined with a k- ϵ turbulence closure model. The additional bottom shear stress effects were included into the momentum equations using the formulae of Karambas (1998). The governing equations in two-dimensional domain can be given as follows:

$$\frac{\partial \theta \mathbf{u}}{\partial \mathbf{x}} + \frac{\partial \theta \mathbf{v}}{\partial \mathbf{v}} = 0 \tag{1}$$

$$\frac{\partial \theta u}{\partial t} + \theta u \frac{\partial \theta u}{\partial x} + \theta v \frac{\partial \theta u}{\partial y} = \theta \frac{\partial}{\partial x} \left[2(v + v_t) \frac{\partial \theta u}{\partial x} \right] + \theta \frac{\partial}{\partial y} \left[(v + v_t) \left(\frac{\partial \theta u}{\partial y} + \frac{\partial \theta u}{\partial x} \right) \right] - \frac{\theta}{\rho} \frac{\partial p}{\partial x} - \frac{\tau_{bx}}{\rho} \tag{2}$$

$$\frac{\partial \theta v}{\partial t} + \theta u \frac{\partial \theta v}{\partial x} + \theta v \frac{\partial \theta v}{\partial y} = \theta \frac{\partial}{\partial y} \left[2(v + v_t) \frac{\partial \theta v}{\partial y} \right] 1 + \theta \frac{\partial}{\partial x} \left[(v + v_t) \left(\frac{\partial \theta v}{\partial x} + \frac{\partial \theta u}{\partial y} \right) \right] - \frac{\theta}{\rho} \frac{\partial p}{\partial y} - g - \frac{\tau_{by}}{\rho}$$
 (3)

$$\frac{\partial \theta k}{\partial t} + \theta u \frac{\partial \theta k}{\partial x} + \theta v \frac{\partial \theta k}{\partial y} = \frac{\partial}{\partial x} \left[\left(v + \frac{v_{_t}}{\sigma_{_k}} \right) \frac{\partial \theta k}{\partial x} \right] + \frac{\partial}{\partial y} \left[\left(v + \frac{v_{_t}}{\sigma_{_k}} \right) \frac{\partial \theta k}{\partial y} \right] p_{_r} - \epsilon \tag{4}$$

$$\frac{\partial \theta \epsilon}{\partial t} + \theta u \frac{\partial \theta \epsilon}{\partial x} + \theta u \frac{\partial \theta \epsilon}{\partial y} = \frac{\partial}{\partial x} \left[\left(v + \frac{v_t}{\sigma_g} \right) \frac{\partial \theta \epsilon}{\partial x} \right] + \frac{\partial}{\partial y} \left[\left(v + \frac{v_t}{\sigma_g} \right) \frac{\partial \theta \epsilon}{\partial y} \right] + C_{\text{sl}} (P_r) \frac{\epsilon}{k} - C_{\text{s2}} \epsilon \frac{\epsilon}{k}$$
 (5)

$$P_{r} = v_{t} \left[2 \left(\frac{\partial \theta u}{\partial x} \right)^{2} + 2 \left(\frac{\partial \theta v}{\partial y} \right)^{2} + \left(\frac{\partial \theta u}{\partial y} + \frac{\partial \theta v}{\partial x} \right)^{2} \right]$$
 (6)

$$\mathbf{v}_{t} = \mathbf{C}_{d} \frac{\mathbf{k}^{2}}{\mathbf{s}} \tag{7}$$

where, t is time, u and v are the mean velocity components in x and y direction, respectively, p is the mean pressure and g is the vertical gravity acceleration, ρ is the density of the fluid, v and v_t are, respectively the fluid and eddy viscosities, k is the turbulence kinetic energy, P_r is the production of turbulence kinetic energy, ϵ is the turbulence dissipation rate, θ is the partial cell treatment parameters, τ_{bx} and τ_{by} are the bottom shear stresses. The model constants were set according to Launder and Spalding (1974) and are presented in Table 1. The bottom shear stresses were estimated from Karambas (1998):

$$\frac{\tau_{bx}}{\rho} = \frac{f_w}{2} u_b \sqrt{u_b^2 + v_b^2} \tag{8a}$$

$$\frac{\tau_{bx}}{\rho} = \frac{f_w}{2} u_b \sqrt{u_b^2 + v_b^2} \tag{8b}$$

where, u_b and v_b are the horizontal and vertical components of the near bottom velocity and f_w is the friction coefficient.

Boundary conditions: The Volume Of Fluid (VOF) method (Hirt and Nichols, 1981) was used to solve the free surface boundary. This method tracks the free surface motion by solving a volume of fluid function, F which has value in a range of $0 \le F \le 1$, in the following transport equation:

$$\frac{\partial \theta F}{\partial t} + \theta u \frac{\partial F}{\partial x} + \theta v \frac{\partial F}{\partial y} = 0 \tag{9}$$

Table 1: Constants of the k- ϵ turbulence closure model (Launder and Splading, 1974)

Parameters	Values
$\overline{\mathrm{C}_{\mathtt{d}}}$	0.09
$\mathrm{C}_{\mathfrak{s}1}$	1.44
$\mathrm{C}_{\scriptscriptstyle{c2}}$	1.92
σ_k	1.00
σ_{c}	1.30

At the inflow boundary, the Dirichlet-type wave generator and the weakly reflecting boundary (Petit *et al.*, 1994) were applied as follows:

$$\frac{\partial \varphi}{\partial t} - C \frac{\partial \varphi}{\partial x} = \frac{\partial \varphi_i}{\partial t} - C \frac{\partial \varphi_i}{\partial x} \tag{10}$$

where, φ_i is the variables of incident wave signals and φ is for the computed variables including the free surface displacement and velocities. The structure of breakwater was placed at the other end of numerical domain. The partial cell treatment technique of NASA-VOF2D code (Torrey et al., 1985) was adopted into the present model to create internal obstacles as the representation of breakwater structure inside the numerical domain. No-slip rigid wall was taken as the boundary conditions at the bottom and along the solid boundary of the breakwater structure.

An assumption for zero vertical fluxes of k and ϵ was taken as the turbulence boundary conditions at the free surface:

$$\frac{\partial k}{\partial n} = 0, \quad \frac{\partial \epsilon}{\partial n} = 0 \tag{11}$$

The Neumann continuative boundary condition was defined at the inflow of turbulence boundary:

$$\left(\frac{\partial k}{\partial x}\right)_{x=0} = 0, \quad \left(\frac{\partial \epsilon}{\partial x}\right)_{x=0} = 0 \tag{12}$$

and no-slip rigid wall without turbulent boundary layer was assumed at the bottom and along the solid boundaries.

Initial conditions: The calculation started with zero velocity and hydrostatic pressure for fluid field and flat bed profile was initialized at y = 0 m at the bottom. The initial conditions for the turbulence field were set according to Lin and Liu (1998) and Bakhtyar *et al.* (2009) as follows:

$$k = \frac{1}{2}u_t^2, \quad u_t = \delta C, \quad \delta = 0.0025$$
 (13)

$$\varepsilon = C_{\mu} \frac{k^2}{v_t}, \quad v_t = \varepsilon v, \quad \varepsilon = 0.1$$
 (14)

where, C is the wave celerity at the inflow boundary, C_{μ} is an empirical coefficient as given in Table 1.

Cross-shore sediment transport model: An empirical sediment transport formula of Bailard (1981) was used for sediment transport prediction. The sediment particles were assumed to be non-cohesive. The formula of total volumetric sediment transport rate, S(t) is presented below:

$$\langle S(t) \rangle = \langle S_{b}(t) \rangle + \langle S_{s}(t) \rangle \tag{15}$$

$$\left\langle S_{b}(t)\right\rangle = \frac{\rho c_{f} \epsilon_{b}}{(\rho_{s} - \rho)g(1 - p)\tan\phi} \cdots \left\{ \left\langle \left|u_{b}(t)\right|^{2} u_{b}(t)\right\rangle - \frac{\tan\alpha}{\tan\phi} \left\langle \left|u_{b}(t)^{3}\right|\right\rangle \right\}$$

$$(16)$$

$$\left\langle S_{s}(t)\right\rangle = \frac{\rho c_{f} \varepsilon_{s}}{(\rho_{s} - \rho) g(1 - p) w} \cdots \left\{ \left\langle \left|u_{b}(t)\right|^{3} u_{b}(t)\right\rangle - \frac{\varepsilon_{s}}{w} \tan \alpha \left\langle \left|u_{b}(t)^{5}\right|\right\rangle \right\}$$

$$(17)$$

where, $S_b(t)$ and $S_s(t)$ are the instantaneous volumetric sediment transport rate for bed-load and suspended load, respectively; g is the gravity acceleration, ρ is the density of the fluid, ρ_s is the density of sediment, w is the fall velocity of sediment, ε_b and ε_s are the bed-load and suspended-load efficiency factors, respectively, c_f is the drag coefficient of the bed, p is the sediment porosity, φ is the angle of repose, α is the bed-slope angle, $u_b(t)$ is the instantaneous near bottom fluid velocity and <> is for time-average; Table 2 presents the parameters used in the current simulation. In the Bailard's original equation, it was recommended to use a value of c_f = 0.005. While in the present study, 0.5 f_w was used to replace c_f , in which the skin friction factor, f_w which is formulated based on Jonsson (1966) as follows:

$$f_w = \exp\left(5.213 \left(\frac{a_o}{r}\right)^{-0.194} - 5.977\right), \dots for \frac{a_o}{r} \ge 1.59$$
 (18a)

$$f_w = 0.3, \quad \text{for } \frac{a_o}{r} < 1.59$$
 (18b)

where, r is the bed roughness that assumed as equal to D_{50} and a_o is the amplitude of orbital motion at the bottom, for the first order linear wave theory:

$$a_o = \frac{H}{2\sinh\left(\frac{2\pi d}{L}\right)} \tag{19}$$

The change of bed profile was calculated by the continuity equation for sediment according to Fredsoe and Deigaard (1992) as follows:

$$\frac{\partial \langle \mathbf{y} \rangle}{\partial t} + \frac{1}{(1-\mathbf{p})} \frac{\partial \langle \mathbf{S}(t) \rangle}{\partial \mathbf{x}} = 0 \tag{20}$$

where, y is the bed level and p is the porosity of sediment.

The finite difference method was used to solve the six unknown variables in Eq. 1-7 and 9; u, v, p, F, k and ϵ . The solutions were solved in a staggered grid. The Simple Implicit Method for Pressure-Linked Equations (SIMPLE) algorithm proposed by Patankar (1980) was used as the solution of RANS equations. The VOF equation was solved using the donor-acceptor algorithm (Hirt and Nichols, 1981).

Table 2: Test conditions for the validation of scour/deposition pattern

Breakwater	d (m)	H (m)	L (m)	T(s)	$D_{50}(\mu m)$
Vertical	0.3	0.05	1.714	1.17	150

MODEL VALIDATION

The numerical results were validated by using experimental data of Xie (1981) and Zhang et al. (2001) for the near-bottom horizontal velocity. The numerical results were also compared with an analytical solution of standing waves that is based on the second order theory of Miche. To ensure the validity of numerical results, 14 different tests were performed with parameters ranging from 0.01-0.67 for the wave steepness and 0.05-0.24 for the relative depth. These simulations were also performed in three different water depths of 0.3, 0.5 and 0.65 m. Among the fourteen tests, three of them based on the experiment of Zhang et al. (2001) were performed with including the overtopping process.

Figure 1 shows the comparisons of the near bottom horizontal velocity data (U_{max}) between the numerical, analytical and experimental results. Figure 1a and b show the values of U_{max} measured at the first node of standing waves (x = L/4) formed in front of the breakwater while 1(c) and 1(d) for the U_{max} values measured at halfway between the first node and antinode of standing waves (x = L/8). From these plots, it has been calculated that the values of coefficient correlation in all these comparisons are higher than 0.9, $R^2 = 0.910$ for Fig. 1a, $R^2 = 0.918$ for Fig. 1b, $R^2 = 0.972$ for Fig. 1c and $R^2 = 0.973$ for Fig. 1d. These results indicate that the numerical results are in a very good agreement either with the experimental data or with the theoretical results. The numerical results at x = L/8 has a better accuracy than at the first node.

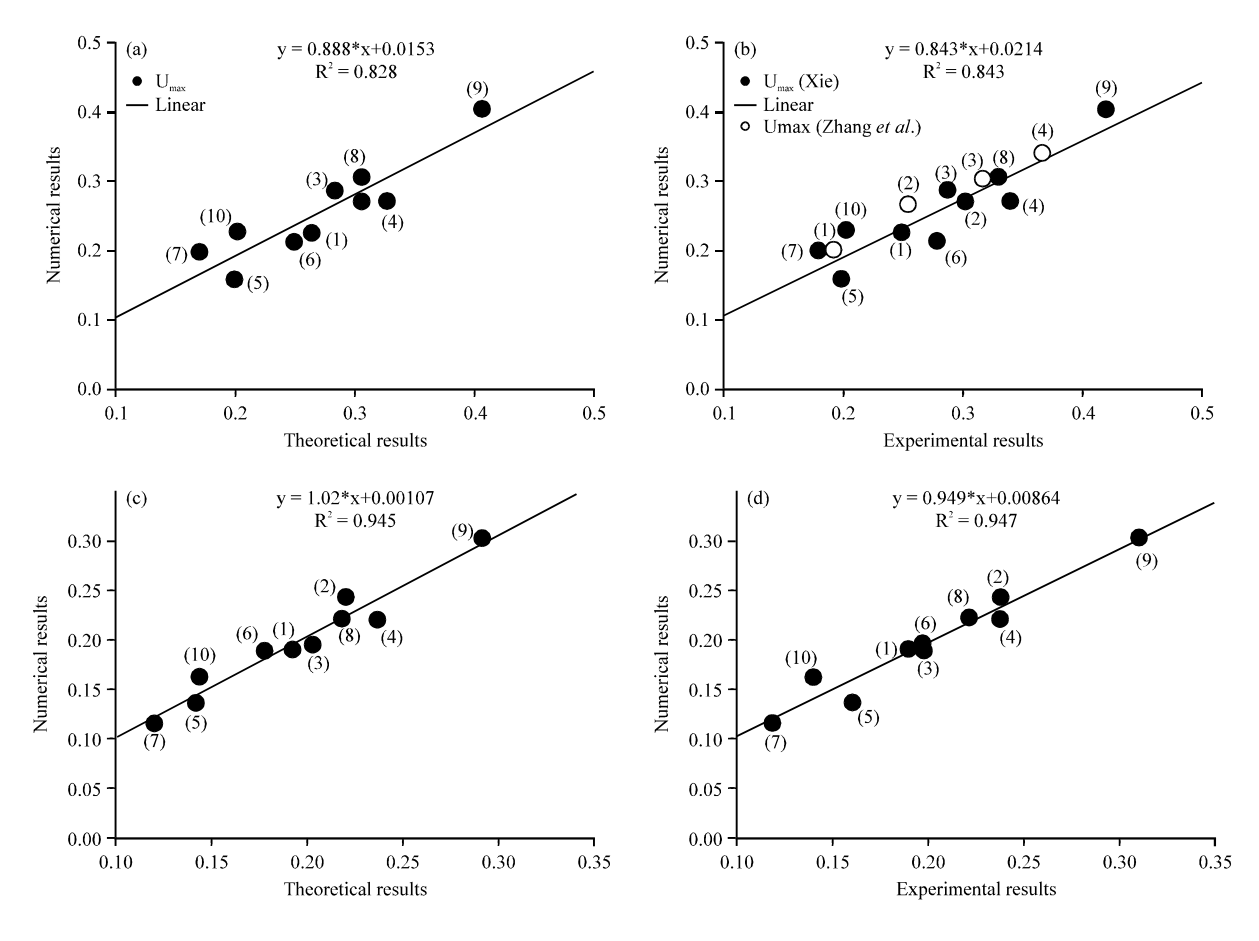


Fig. 1(a-d): Comparison of maximum horizontal orbital velocities, (a) Numerical vs. theoretical at the 1st node (x = L/4), (b) Numerical vs. experimental at the 1st node (x = L/4), (c) Numerical vs. theoretical at x = L/8 and (d) Numerical vs. experimental at x = L/8

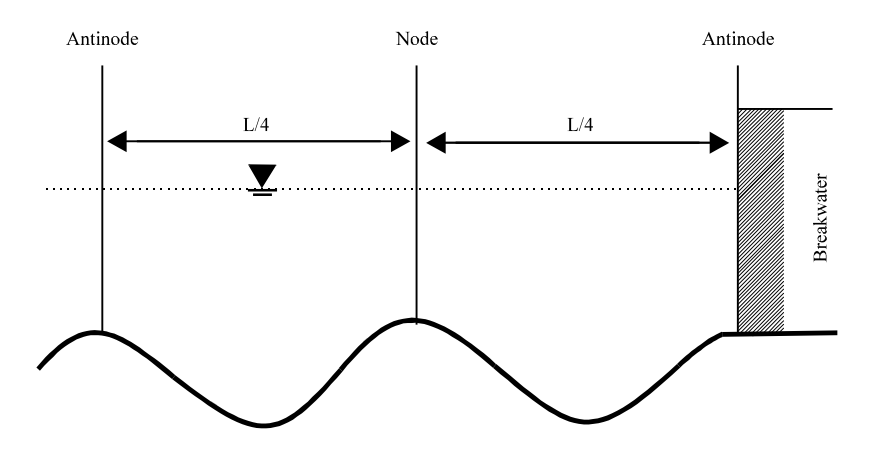


Fig. 2: Scour/deposition pattern for coarse material (Xie, 1981)

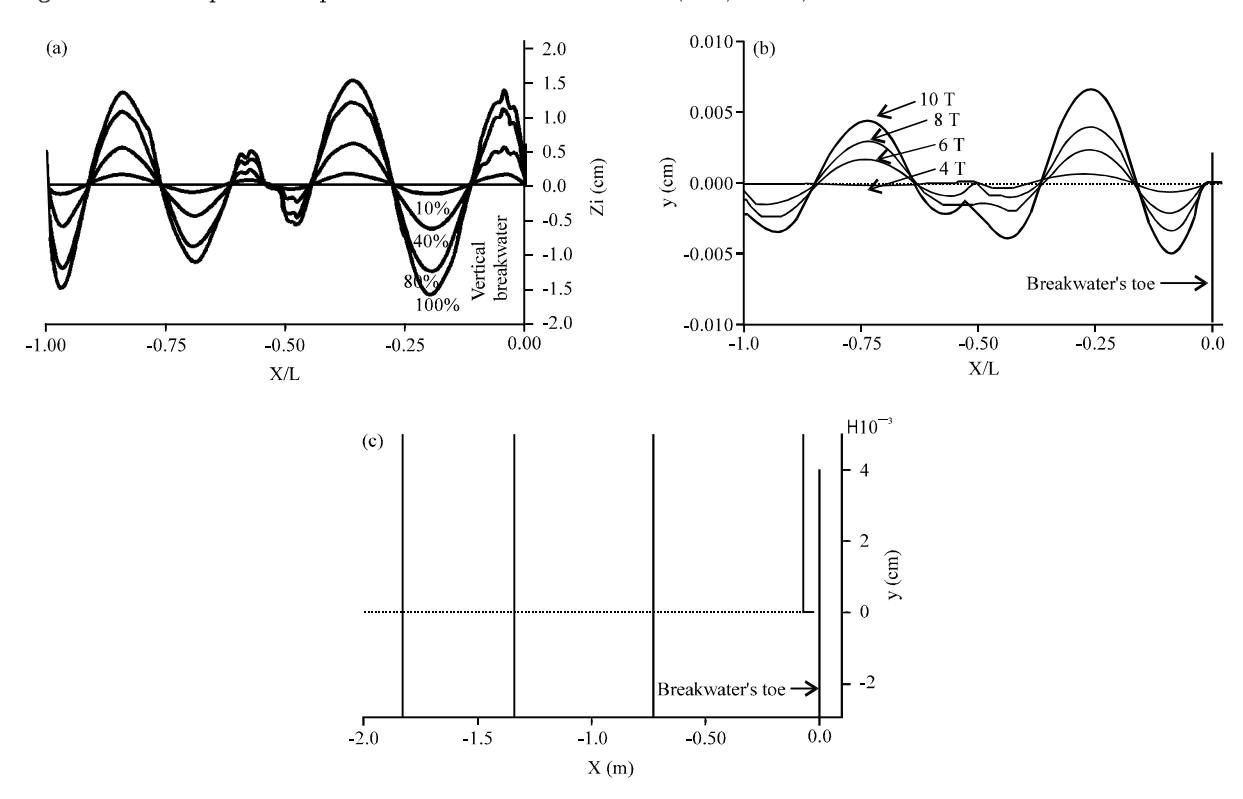


Fig. 3(a-c): Scour/deposition patterns (a) Numerical simulations of Tahersima *et al.* (2011)-equilibrium state, (b) Present model-no equilibrium state (duration: 10T) and (c) Present model result without bottom shear stress calculation-unstable result

The scouring/deposition pattern of present model was compared to the numerical simulation of Tahersima *et al.* (2011). The test conditions for this comparison were taken from the experiment of (Xie, 1981, experiment No. 11a, Table 1) and are given in Table 2. Xie observed that the type of scouring pattern of this test condition is categorized as coarse material and the pattern is schematized in Fig. 2 (Xie, 1981).

The scour/deposition patterns of the both models are presented in Fig. 3 in which the x-axis is normalized by the wavelength (L). As shown in Fig. 3(a), the scour/deposition pattern of

Tahersima *et al.* (2011) is quite misleading, not following the Xie's pattern for coarse material (Fig. 2). Meanwhile, the scour/deposition pattern of the present model (Fig. 3b) is accurately similar to the Xie's pattern. The scour troughs are located under the halfway (L/8 from the breakwater) and the deposition ridges occur under the node (L/4 from the breakwater) of standing wave.

An additional test found that the terms of bottom shear stress are required in the momentum equations to produce physical bed profile when applying the Bailard's formula. Without these terms, the present model produced an unphysical bed profile as shown in Fig. 3c. The misleading pattern of Tahersima *et al.* (2011) might be caused they did not take into account the bottom shear stress effect in the calculation.

RESULTS AND DISCUSSION

The focus of this study is to show application of the present model to investigate the effects of different wave conditions on scouring pattern in front of an impermeable breakwater. Four numerical experiments were conducted by varying the size of incoming waves in the same numerical wave flume with size of 8.5 m in length, 0.6 m in height and the distance between wave generator and the breakwater's toe is 6.05 m. The wave parameters are presented in Table 3 while the characteristics of sediment used in the simulation are given in Table 4. The numerical domain was descritized using the grid size of $\Delta x = 0.05$ m and $\Delta y = 0.025$ which means there are 170 cells in the direction and 24 cells in the direction. All simulations were performed for 24.1s or equal to 10 wave periods.

Interactions between the incident waves and reflected waves that occur periodically will create fully standing waves in front of the vertical breakwater. The first group (Test 1 and 2) is different to the second group (Test 3 and 4) in terms of the length of incoming waves which is shorter than the waves used in the second group. It is observed that the development of standing waves in these two groups occur in different times.

Figure 4 shows the free surface profile in the four cases as the water surface at its maximum and minimum extreme positions. In every wave period, these extreme positions are attained twice which are at 3 T, 3.5 T, 4 T...9 T and 9.5 T for Test 1 and 2 while at 3.25 T, 3.75 T, 4.25 T...9.25 T and 9.75 T for Test 3 and 4. The fully standing waves indicated by a series of nodes

Table 3: Wave parameters for simulations

Test No.	T (s)	L (m)	H (m)	d (m)
1	1.53	2.4	0.050	0.3
2	1.53	2.4	0.085	0.3
3	2.41	4.0	0.050	0.3
4	2.41	4.0	0.090	0.3

Table 4: Sediment properties

Parameters	Values
φ	31.00°
ϵ_{b}	0.10
$\epsilon_{\rm s}$	0.02
$\rho_s (\text{kg m}^{-3})$	2650.00
$ ho_s (kg m^{-3})$ $ m w (m sec^{-1})$	0.02
D_{50} (mm)	0.44
p	0.40

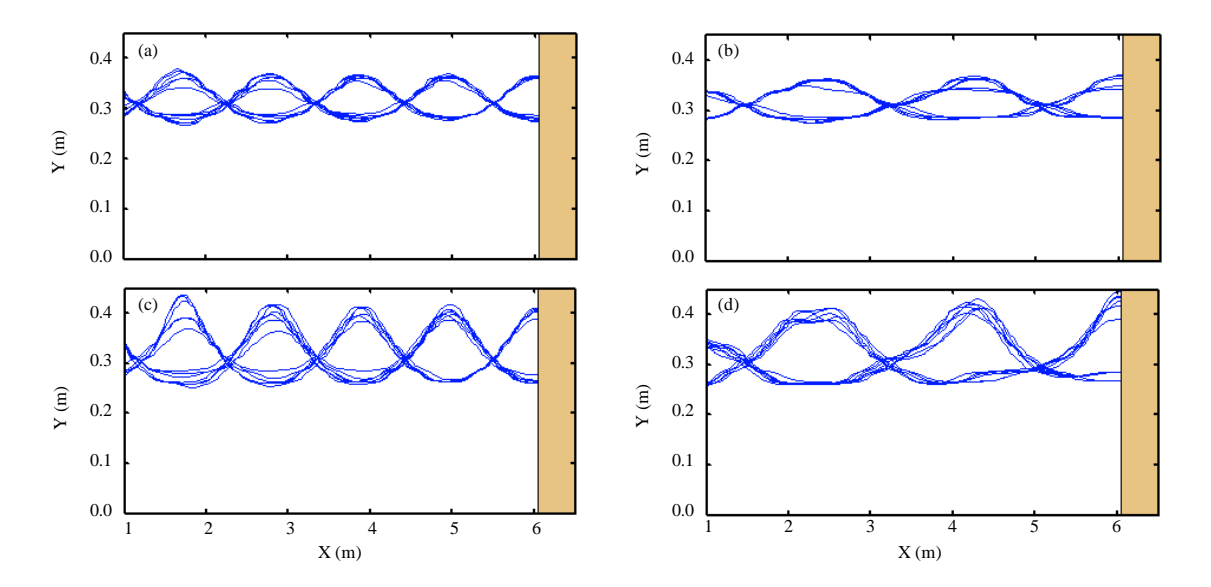


Fig. 4(a-d): Free surface profile of the standing waves in front of vertical breakwater for different parameters of the incoming waves, (a) Test 1, (b) Test 2, (c) Test 3 and (d) Test 4

and antinodes form in all test cases and they are all well simulated by the present model. It is also observed that for the tests in the different groups the nodes and antinodes form at different locations while they form at the same locations for the tests in a same group.

The resultant amplitude and the size of standing waves become higher and bigger with the increasing of wave height and wave length, respectively. Different wave characteristics observed in all test cases will have correlations and direct impacts to the scouring pattern that form at the bottom, as will be discussed below.

After analyzing the characteristics of sediment using the non-dimensional parameter, U_{max} - U_{cr} /w as introduced by Xie (1981), it was found that the sediment used for the present simulation is categorized as coarse material. So then, according to Xie (1981), they respond more on the bottom re-circulating cells and are mainly transported in the bed-load mode. It is expected that the scouring pattern will follow the pattern in Fig. 2.

The effects of different wave conditions on the scouring pattern can be observed in Fig. 5 that shows the evolution of bed profile during 10 wave periods for all test cases. In all cases, the scouring depth and deposition height increase with the increasing of time. By relating Fig. 4 and 5, it can be seen the correlations between the characteristics of standing waves and scouring pattern at the bottom. It is observed that for all cases the scouring troughs occur at the halfway between nodes and antinodes while the deposition ridges form under the nodes. In the first group (Test 1 and 2), as observed in Fig. 4a and b, the 1st node and 2nd antinode that form in front of breakwater are located at 5.5 and 5 m, respectively, from the left boundary. In Fig. 5a and b, the 1st ridge occurs exactly at the same locations where the 1st node form and the troughs occur around the 2nd antinode. The same patterns can also be observed for the second group (Test 3 and 4).

In the first group, the distances between one deposition ridges to the others are closer than in the second group, resembling the distances between nodes of standing waves. In each group, as the wave height increases the scouring depth and deposition height also increases. While by comparing the two groups, it can be seen that the size of scouring troughs and deposition ridges in the second

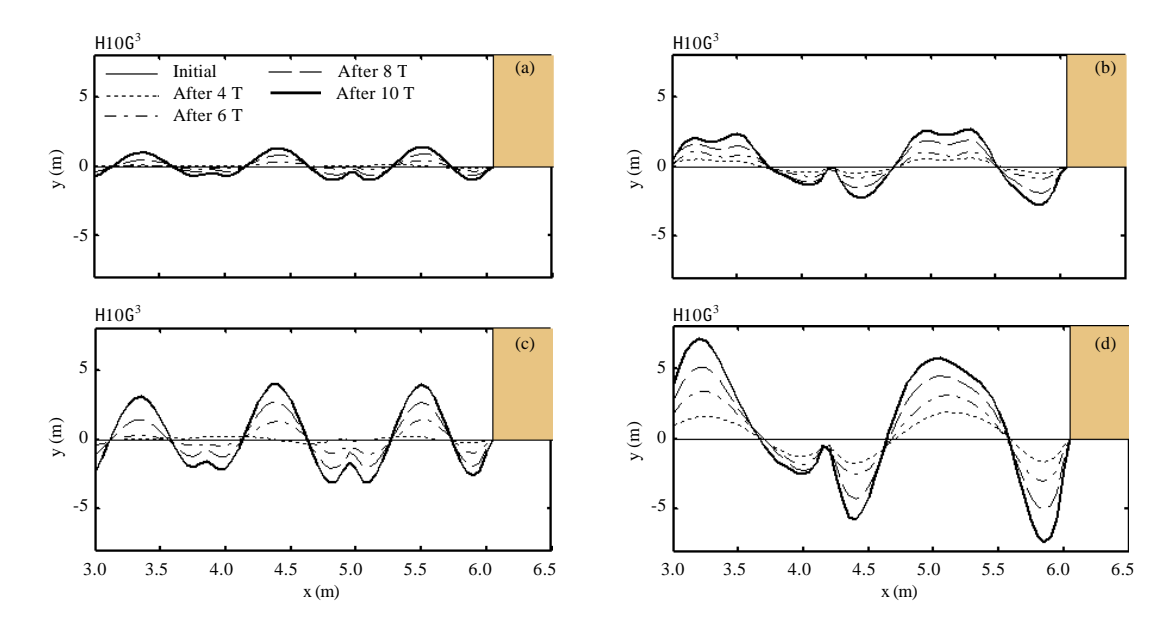


Fig. 5(a-d): Evolution of numerical bed-profile during 10 wave periods of simulation, (a) Test 1, (b) Test, (c) Test 3 and (d) Test 4

group are larger than in the first group as the consequences of longer wave length. Waves with bigger size carry higher energy that will induce stronger flow under the surface that eventually gives more impacts to sediment movement at the bottom. This explains why the scouring depth and deposition height in Test 3 are deeper and higher than in Test 1, although the wave height in both tests is similar. It is because of the wave length in Test 3 longer than in Test 1.

It is interesting to compare the bed level under the 2nd antinode of Test 2, 3 and 4. In Test 2, although it is higher than the area around the 2nd antinode, the bed-level exactly under the 2nd antinode is scoured from its initial level. However, it does not occur in Test 3 and 4. It is also interesting to compare the maximum scouring depth between the two groups. Based on the data of present study, maximum scouring depth for the first group occurs at the troughs around the 2nd antinode. While for the second group, it occurs right in front of the breakwater's toe. All these differences in the bed profile characteristics are expected appearing due to different characteristics of re-circulating cells above the bed which is known as the key mechanism that induce scouring at the bottom.

CONCLUSION

A two dimensional RANS-VOF based numerical model has been developed for scouring simulation in front of impermeable vertical breakwaters. An empirical sediment transport formulae of Bailard (1981) was coupled with the hydrodynamics model. The additional bottom shear stress terms were included in the momentum equations using the formulae of Karambas (1998). These terms are necessary to produced physical scouring/deposition patterns.

Validation results of the near bottom velocity showed that the present model is very accurate for predicting the near bottom velocity. The predicted scouring/deposition patterns can resemble the scouring/deposition pattern of coarse material of Xie (1981) better than the previous study. Based on the results of the present numerical experiments, the following information can be taken:

- Information of the locations where nodes and antinodes of standing waves form is very important to facilitate the analysis of scouring pattern at the bottom
- Different wave conditions will produce different characteristics of standing waves in front of
 the vertical breakwater in terms of the locations of nodes and antinodes, size of the resultant
 amplitude and width of the resultant standing waves. The resultant amplitude and width of
 the standing waves increase with the increasing of wave height and wave length
- Different characteristics of standing waves on the surface have strong correlations to the scouring/deposition pattern at the bottom. The scouring depth and deposition ridge increase with the increasing of time. As the wave height and wave length increase the size scouring depth and deposition height also increase

ACKNOWLEDGMENTS

The author would like to thank the Minister of Higher Education (MoHE) Malaysia for financially supporting this study project through Research Grant of Tabung Amanah MLNG-INOS (TE 67901).

REFERENCES

- Bailard, J.A., 1981. An energetics total load sediment transport model for a plane sloping beach. J. Geophys. Res., 86: 10938-10954.
- Bakhtyar, R., D.A. Barry, A. Yeganeh-Bakhtiary and A. Ghaheri, 2009. Numerical simulation of surf-swash zone motions and turbulent flow. Adv. Water Res., 32: 250-263.
- Engelund, F.A. and J. Fredsoe, 1976. A sediment transport model for straight alluvial channels. Nordic Hydrol., 7: 293-306.
- Fredsoe, J. and J. Deigaard, 1992. Mechanics of Coastal Sediment Transport. World Scientific, Singapore, ISBN-13: 9789810208417, Pages: 369.
- Gislason, K., J. Fredsoe and B.M. Sumer, 2009. Flow under standing waves: Part 2. Scour and deposition in front of breakwaters. Coastal Eng., 56: 363-370.
- Hajivalie, F. and A. Yeganeh-Bakhtiary, 2009. Numerical study of breakwater steepness effect on the hydrodynamics of standing waves and steady streaming. J. Coastal Res., 56: 658-662.
- Hajivalie, F., A. Yeganeh-Bakhtiary, H. Houshanghi and H. Gotoh, 2012. Euler-lagrange model for scour in front of vertical breakwater. Applied Ocean Res., 34: 96-106.
- Hirt, C.W. and B.D. Nichols, 1981. Volume of Fluid (VOF) method for the dynamics of free boundaries. J. Comput. Phys., 39: 201-225.
- Irie, I. and K. Nadaoka, 1984. Laboratory reproduction of seabed scour in front of breakwaters. Proceedings of the 19th International Conference on Coastal Engineering, September 3-7, 1984, Houston, TX., pp: 1715-1731.
- Jonsson, I.G., 1966. Wave boundary layers amd friction factors. Proceedings of 10th Conference on Coastal Engineering, (CE'66), Tokyo, Japan, pp. 127-148.
- Karambas, T.V., 1998. 2DH non-linear dispersive wave modelling and sediment transport in the nearshore zone. Coastal Eng., 26: 2940-2953.
- Launder, B.E. and D.B. Spalding, 1974. The numerical computation of turbulent flows. J. Comput. Mech. Appl. Mech. Eng., 3: 269-289.
- Lin, P. and P.L.F. Liu, 1998. A numerical study of breaking waves in the surf zone. J. Fluid Mech., 359: 239-264.

- Nichols, B.D., C.W. Hirt and R.S. Hotchkiss, 1980. SOLA-VOF: A solution algorithm for transient fluid flow with multiple free boundaries. http://www.ewp.rpi.edu/hartford/~ernesto/F2012/CFD/Readings/SOLA-VOF-1980-P1.pdf
- Patankar, S.V., 1980. Numerical Heat Transfer and Fluid Flow. McGraw-Hill, New York, USA.
- Petit, H.A.H, M.R.A. van Gent and P. van den Bosch, 1994. Numerical simulation and validation of plunging breakers using a 2D navier-stokes model. Proceedings of the 24th International Coastal Engineering Conference, October 23-28, 1994, Kobe, Japan, pp: 511-524.
- Sumer, B.M., R.J.S. Whitehouse and A. Torum, 2001. Scour around coastal structures: A summary of recent research. Coastal Eng., 44: 153-190.
- Tahersima, M., A. Yeganeh-Bakhtiary and F. Hajivalie, 2011. Scour pattern in front of vertical breakwater with overtopping. J. Coastal Res., 64: 598-602.
- Takahasi, S., 2002. Design of vertical breakwaters. Proceedings of the 28th International Conference on Coastal Engineering, July 7-12, 2002, Cardiff, Wales.
- Torrey, M.D., L.D. Cloutman, R.C. Mjolness and C.W. Hirt, 1985. NASA-VOF2D: A computer program for incompressible flows with free surfaces. Report No. LA-10612-MS, Los Alamos Scientific Laboratory, Los Alamos, NM., USA.
- Xie, S.L., 1981. Scouring patterns in front of vertical breakwaters and their influences on the stability of the foundation of the breakwaters. Master Thesis, Department of Civil Engineering, Delft University of Technology, Delft Netherlands.
- Zhang, S., A. Cornett and Y. Li, 2001. Experimental study of kinematic and dynamical characteristics of standing waves. Proceedings of the 29th IAHR Conference, September 16-21, 2001, Beijing, China.